Downregulation of microRNA-199a-5p attenuates hypoxia/reoxygenation-induced cytotoxicity in cardiomyocytes by targeting the HIF-1α-GSK3β-mPTP axis

DA-WEI LIU[1,2], YA-NAN ZHANG[1], HAI-JUAN HU[1], PU-QIANG ZHANG[1] and WEI CUI[1]

[1]Department of Cardiology, Second Hospital of Hebei Medical University and Hebei Institute of Cardiovascular Research, Shijiazhuang, Hebei 050011; [2]Department of Cardiology, Workers' Hospital of Tangshan, Tangshan, Hebei 063000, P.R. China

Received September 6, 2018; Accepted April 3, 2019

DOI: 10.3892/mmr.2019.10197

Abstract. MicroRNAs (miRs) have been identified as critical regulatory molecules in myocardial ischemia/reperfusion injury; however, the exact expression profile of miR-199a-5p in reperfusion injury and the underlying pathogenic mechanisms remain unclear. In the present study, it was revealed that miR-199a-5p expression was significantly increased in the plasma of patients with acute myocardial infarction and in a H9c2 cell model of oxygen-glucose deprivation and reperfusion (OGD/R) via reverse transcription-quantitative PCR. H9c2 cells were transfected with miR-199a-5p mimic or inhibitor, or short interfering RNA (siRNA) specific to hypoxia-inducible factor-1α (HIF-1α). MTS, lactate dehydrogenase (LDH), TUNEL staining and flow cytometry assays were performed to determine the proliferation, LDH activity, apoptosis and mitochondrial membrane potential (ΔΨm) of H9c2 cells, respectively. The overexpression of miR-199a-5p in the OGD/R cell model significantly decreased the viability and increased the lactate dehydrogenase leakage of cells; whereas knockdown of miR-199-5p induced the opposing effects. Additionally, inhibition of miR-199-5p significantly attenuated OGD/R-induced alterations to the mitochondrial transmembrane potential (ΔΨm) and increases in the apoptosis of cells. Furthermore, the overexpression or knockdown of miR-199a-5p decreased or increased the expression of HIF-1α and phosphorylation of glycogen synthase kinase 3β (GSK3β) in OGD/R-treated H9c2 cells. Additionally, siRNA-mediated downregulation of HIF-1α decreased phosphorylated (p)-GSK3β (Ser9) levels and reversed the protective effects of miR-199a-5p inhibition on OGD/R-injured H9c2 cells. Similarly, treatment with LiCl (a specific inhibitor of p-GSK3β) also attenuated the protective effects of miR-199a-5p knockdown on OGD/R-injured H9c2 cells. Mechanistic studies revealed that HIF-1α was a target of miR-199a-5p, and that HIF-1α downregulation suppressed the expression of p-GSK3β in OGD/R-injured H9c2 cells. Furthermore, an miR-199a-5p inhibitor increased the interaction between p-GSK3β and adenine nucleotide transferase (ANT), which was decreased by OGD/R. Additionally, miR-199a-5p inhibitor reduced the OGD/R-induced interaction between ANT and cyclophilin D (Cyp-D), potentially leading to the increased mitochondrial membrane potential in inhibitor-transfected OGD/R-injured H9c2 cells. Collectively, the present study identified a novel regulatory pathway in which the upregulation of miR-199a-5p reduced the expression of HIF-1α and p-GSK3β, and potentially suppresses the interaction between p-GSK3β and ANT, thus promoting the interaction between ANT and Cyp-D and potentially inducing cytotoxicity in OGD/R-injured H9c2 cells.

Correspondence to: Dr Wei Cui, Department of Cardiology, Second Hospital of Hebei Medical University and Hebei Institute of Cardiovascular Research, 361 Zhongshan East Road, Shijiazhuang, Hebei 050011, P.R. China
E-mail: cuiwei@medmail.com.cn

Key words: microRNA-199a-5p, myocardial ischemia/reperfusion injury, hypoxia-inducible factor-1α, glycogen synthase kinase 3β, cytotoxicity

Introduction

At present, acute myocardial infarction (AMI) remains a major cause of mortality globally (1). Timely and effective reperfusion significantly decreases mortality (2); however, reperfusion can result in myocardial injury, inducing myocardial apoptosis and cardiac contractile dysfunction (3). Various studies have suggested that cardiac ischemia/reperfusion (I/R) resulting in oxidative damage (4), inflammation (5) and cardiac dysfunction (6) leads to cardiac dysfunction and arrhythmia. Thus, the pathogenic mechanisms underlying reperfusion injury have received substantial attention.

MicroRNAs (miRNAs/miRs) are small noncoding RNAs that are ~17-27 nucleotides in length, which can suppress gene expression via translational repression and transcript cleavage (7). miRNAs serve important roles in regulating cardiac function, including heart-muscle contraction, conducting electrical signals, heart morphogenesis and I/R injury pathways (8). A number of miRNAs have been identified as aberrantly expressed following cardiac I/R, including miR-1 (9), miR-15 (10), miR-92a (11), miR-320 (12) and

miR-494 (13); however, the underling mechanisms remain unclear.

Recent studies reported that miR-199a-5p is a regulator of cardiac remodeling, ventricular hypertrophy, status epilepticus and heart failure (14,15). Our recent study reported that atorvastatin attenuated the apoptosis of I/R-induced cardiomyocytes by regulating the miR-199a-5p-mediated expression of glycogen synthase kinase 3β (GSK3β); however, our research also revealed that GSK3β was not a target of miR-199a-5p, indicating that other molecules downstream of miR-199a-5p regulated GSK3β signaling (16). Hypoxia-inducible factor-1α (HIF-1α) is involved in the regulation of GSK3β signaling in H9c2 cells in myocardial I/R injury (17); however, the association between miR-199a-5p, HIF-1α and GSK3β signaling and proapoptotic molecular mechanisms remain unknown.

The present study demonstrated that the upregulation of miR-199a-5p reduced the viability of, and promoted lactate dehydrogenase (LDH) release from rat cardiomyocyte H9c2 cells during oxygen-glucose deprivation and reperfusion (OGD/R). It was hypothesized that miR-199a-5p downregulation may protect H9c2 cardiomyocytes against I/R-induced mitochondrial permeability transition pore (mPTP) opening. Furthermore, a regulatory role for HIF-1α and GSK3β in mPTP opening was identified, potentially contributing to OGD/R-induced cell apoptosis. Additionally, the effects of miR-199a-5p downregulation on apoptosis, mPTP opening, p-GSK3β signaling and HIF-1α expression were determined.

Materials and methods

Reagents. DMEM, FBS and antibiotics (penicillin and streptomycin) were purchased from Gibco (Thermo Fisher Scientific, Inc.). HIF-1α (cat.no.20960-1-AP), GSK3β (cat.no.22104-1-AP), phosphorylated (p)-GSK3β (cat. no. 14850-1-AP), adenine nucleotide transferase (ANT; cat. no. 17796-1-AP), cyclophilin D (Cyp-D; cat. no. 12716-1-AP) and β-actin antibodies (cat. no. 60008-1-Ig) were purchased from ProteinTech Group, Inc. Transfection of H9c2 cells was performed using HiPerFect Transfection Reagent (Qiagen, Inc.). miR-199a-5p mimic and inhibitor were obtained from Sigma-Aldrich (Merck KGaA). SuperScript® VILO™ cDNA Synthesis and SYBR-Green qPCR Super Mix UDG kits were obtained from Invitrogen (Thermo Fisher Scientific, Inc.).

Patients and specimens. A total of 19 male patients with AMI (range: 42-69 age, 55.2±11.8 years) and 20 male patients with unstable angina as control (range: 37-64 age, 51.4±12.9 years), who were admitted to Emergency and Cardiology departments at the Second Hospital of Hebei Medical University between May 2016 and August 2017. Clinical and demographic characteristics of the subjects are presented in Table I. Venous blood samples (5 ml) were centrifuged at ~1,000 x g for 30 min at room temperature, and plasma was stored at -80˚C prior to subsequent analysis. Diagnostic criteria for patients with AMI were previously described (10). Male healthy control samples (n=23) were collected in the study. All subjects provided written informed consent. The present study was approved by the Research Ethics Committee of Second Hospital of Hebei Medical University (Shijiazhuang, China).

H9c2 cells and OGD/R treatment. H9c2 cell (ATCC® CRL-1446™) were purchased from the American Type Culture Collection (ATCC). The cells were cultured at 37˚C in a humidified incubator with 5% CO_2 and 95% air, and maintained in Dulbecco's modified Eagle's medium (DMEM) supplemented with 10% FBS. H9c2 cells were treated with OGD/R or without pre-treatment as previously described with minor modifications (16). Briefly, cells were incubated in glucose-free DMEM and subsequently placed in an anaerobic chamber (95% N_2 and 5% CO_2) at 37˚C for 6 h. Then glucose was added (final concentration 4.5 mg/ml), and cells were incubated under normal growth conditions (95% air and 5% CO_2 for 18 h).

Cell transfection. Prior to transfection, the medium was replaced with DMEM without serum and antibiotics. The miRNA mimic and inhibitor sequences were as follows: miR-199a-5p mimic, 5'-ACAGUAGUCUGCACAUUGGUUA-3'; miR-199a-5p inhibitor, 5'-AGUCUCUCAUAUCUUCGGT-3' and scrambled control (SC), 5'-UUGUACUACACAAAAGUACUG-3'. Following OGD/R treatment, Lipofectamine® 2000 Transfection Reagent was mixed with 50 nM miR-199a-5p mimic, inhibitor, short interfering RNA (siRNA) specific to HIF-1α (si-HIF-1α) or the siRNA negative control (si-NC), and the mixture was added to the cells and incubated for 6 h. Complete medium was then used for culture for 24 h, following which the cells were collected for subsequent experiments. Transfection efficiency was observed and evaluated under the microscope (>70% GFP-positive cells for si-RNA; data not shown) or via quantitative PCR (qPCR) analysis.

siRNA obtained from Merck KGaA was used to knockdown the expression of HIF-1α; si-NC was used as the control. siRNA sequences were as follows: si-NC, 5'-GAGGCATAC AGGGACAACACAGC-3' and si-HIF-1α, 5'-TTGAATCTG GGGGCATGGTAAAAG-3'. siRNA (5 μM) were transfected using Lipofectamine® 2000 (Invitrogen; Thermo Fisher Scientific, Inc.) (18,19). Following mixing of Lipofectamine 2000 with si-HIF-1α or si-NC, the mixture was added to the cells prior to incubation for 6 h. Complete medium was then used; following treatment with lithium chloride (LiCl; 20 mM) for 24 h at 37˚C, which the cells were collected for subsequent experiments.

MTS assay. The viability of cells was determined using the CellTiter 96® AQ_{ueous} One Cell Proliferation Assay kit (Promega Corporation). H9c2 cells ($5x10^3$/well) were seeded in 96-well plates. Following the aforementioned treatments and transfections, 20 μl per 100 μl reagent was added to cells prior to incubation for a further 1 h. The absorbance at 490 nm was detected using a microplate reader.

LDH activity assay. The activity of LDH in the supernatant of treated cells was detected using LDH-Cytotoxicity Assay Kit (cat. no. K311-400; BioVision, Inc.).

Reverse transcription (RT)-qPCR. Total RNA from treated cells and plasma samples were obtained using RNAiso Plus reagent (Takara Bio, Inc.) and TRIzol® LS reagent (Invitrogen; Thermo Fisher Scientific, Inc.), respectively. A total of 0.5 μg RNA from each sample was reverse transcribed into cDNA using the SuperScript® VILO™ cDNA Synthesis kit according

Table I. Clinicopathological characteristics of the 19 patients with AMI and 23 healthy subjects.

Characteristics	AMI (n=19)	Control (n=23)	P-value
Age (years)	55.2±11.8	51.4±12.9	0.326
Hyperlipidemia, n (%)	3 (16)	4 (17)	0.890
Hypertension, n (%)	10 (53)	12 (52)	0.627
SBP (mmHg)	131.1±27	121±19	0.241
DBP (mmHg)	86±22	81±17	0.423
Fasting glucose (mmol/l)	6.14±2.11	5.31±1.79	0.183
DM, n (%)	4 (21)	4 (17)	0.764
WBC ($x10^9$/l)	7.9±2.8	6.5±2.77	0.113
Cr (μmol/l)	91±47.2	67±44.3	0.100
TG (mmol/l)	1.44±0.62	1.32±0.81	0.590
TC (mmol/l)	4.23±0.41	4.11±0.91	0.575
HDL C (mmol/l)	1.03±0.71	1.17±0.54	0.485
LDL C (mmol/l)	2.57±0.9	2.39±0.51	0.445
Current smoking, n (%)	13 (68)	15 (65)	0.826

AMI, acute myocardial infarction; SBP, systolic blood pressure; DBP, diastolic blood pressure; DM, diabetes mellitus; WBC, white blood cell; Cr, creatinine; TG, total triglyceride; TC, total cholesterol; HDL C, high-density lipoprotein cholesterol; LDL C, low-density lipoprotein cholesterol.

to the manufacturer's protocols. RT was conducted at 42˚C for 60 min and 70˚C for 5 min. An SYBR-Green qPCR Super Mix UDG kit (Takara Bio, Inc.) was used for qPCR according to the manufacturer's protocol. PCR was conducted as follows: 95˚C for 2 min, then 40 cycles of 95˚C for 10 sec, 60˚C for 10 sec and 72˚C for 10 sec. The relative expression was calculated using the $2^{-\Delta\Delta Cq}$ formula and normalized to U6 (20). All PCRs were performed in triplicate. The primer sequences were as follows: miR-199a-5p, forward, 5'-CCCAGTGTTCAG ACTACCTGT-3', reverse, 5'-GTGCGTGTCGTGGAG-3'; and U6, forward, 5'-CTCGCTTCGGCAGCACA-3' and reverse, 5'-AACGCTTCACGAATTTGGT-3'.

Western blot analysis. Western blotting was performed as previously described (16). RIPA lysis buffer containing PMSF (Beyotime Institute of Biotechnology) was used to extract total proteins at 4˚C for 30 min. The total protein concentration was determined via a BCA assay. Protein (45 μg) was separated via 12% SDS-PAGE and then transferred onto PVDF membranes (EMD Millipore). Blocking for 1 h at room temperature with 5% non-fat milk in 0.5% TBST (Boster Biological Technology) was followed by incubation overnight at 4˚C with the following primary antibodies: Anti-HIF-1α (1:1,000); anti-GSK3β (1:1,000); anti-p-GSK3β (1:1,000); anti-ANT (1:1,000); anti-Cyp-D (1:1,000) and anti-β-actin (1:1,000). Membranes were washed in PBS with 0.1% Tween-20 and incubated with horseradish peroxidase-conjugated goat anti-mouse IgG and goat anti-rabbit IgG secondary antibodies (1:3,000; cat. nos. ZDR-5307 and ZDR-5306, respectively; OriGene Technologies, Inc. at room temperature for 2 h, according to the manufacturer's protocols. The bonded proteins were visualized with a chemiluminescence detection kit (Clarity Western ECL substrate; Bio-Rad Laboratories, Inc.), and expression was quantified using ImageQuant LAS400 (GE Healthcare Life Sciences).

TUNEL assay. The procedure was conducted using an *in situ* Cell Death Detection kit (Roche Diagnostics) according to the manufacturer's protocols. Nuclei were stained with DAPI (1:2,000; 37˚C for 15 min). TUNEL-positive cells were analyzed as for the immunofluorescent staining described below.

Measurement of mitochondrial membrane potential (ΔΨm). A MitoProbe™ JC-1 Assay kit (Thermo Fisher Scientific, Inc.) was used to measure the ΔΨm according to the manufacturer's protocols. Briefly, following reoxygenation for 6 h, the cells were harvested. The cells in each group were then resuspended in PBS containing 2 μmol/l JC-1 at 37˚C for 30 min with 5% CO_2. Following incubation, the cells were collected and were analyzed using a flow cytometer (Elite Epics; Beckman Coulter, Inc.) with excitation at 488 nm, and emission at 529 nm (monomer form of JC-1, green) and at 590 nm (aggregate form of JC-1, red). The ΔΨm of H9c2 cells in each group was calculated as the fluorescent ratio of red to green. Signals were quantified using ImageJ 2x software (National Institutes of Health).

Immunoprecipitation (IP). IP was performed as previously described (21). In brief, 500 μg of total cellular proteins from the various treatment groups was incubated with 1 μg primary antibodies against ANT and p-GSK3β for 1 h at 4˚C. The mixture was incubated with 20 μl protein A/G PLUS-agarose slurry (Santa Cruz Biotechnology, Inc.) at 4˚C overnight. The pellets were dissolved in 60 μl 1X electrophoresis sample buffer and boiled for 5 min. Samples (30 μl) were analyzed by western blotting as aforementioned.

Cell immunofluorescence assay. Following removal of media, H9c2 cells were fixed and permeated by 4% paraformaldehyde in PBS for 30 min at room temperature, followed by blocking for 25 min at room temperature in 10% goat serum (Dako;

Agilent Technologies, Inc.). The cells were incubated with ANT anti-rabbit IgG (1:50) and p-GSK3β anti-rabbit IgG (1:50) antibody at 4˚C overnight. Samples were then washed with PBS three times and incubated with Alexa Fluor® 594-conjugated anti-rabbit IgG (H+L; 1:150; cat. no. 8889, Cell Signaling Technology, Inc.) for 1 h at room temperature. Nuclei were counter-stained with 100 nM DAPI for 10 min at room temperature. Images were acquired using a confocal microscope (Leica SP5; Leica Microsystems GmbH) and digitized using LAS AF Lite software (versions 2.1 and 2.0; Leica Microsystems GmbH).

Luciferase reporter assay. TargetScan (release 7.1; http://www.targetscan.org/vert_71/) was employed to predict miR-199a-5p targets; HIF-1α was identified as a putative target gene of miR-199a-5p. To construct luciferase reporter vectors, the 3'-untranslated region (3'-UTR) sequence of HIF-1α containing the predicted miR-199a-5p binding sites obtained from rat genomic DNA (50 μg; cat. no. 55704; Celprogen, Inc.) was cloned into a psiCHECK™-2 luciferase reporter vector (cat. no. C8021, Promega) to generate HIF-1α (WT). The mutant (MUT) version of the HIF-1α 3'-UTR lacking complementary with the binding sequence in miR-199a-5p was constructed using a Quick Change Site-Directed Mutagenesis kit [Stratagene; Agilent Technologies, Inc.; HIF-1α (MUT)]. 293A cells (ATCC® CRL-1573™; ATCC) were cultured at 37˚C in a humidified incubator with 5% CO_2 and 95% air, and maintained in DMEM supplemented with 10% FBS and 1% penicillin/streptomycin (100 U/ml; 100 mg/ml) in 24-well plates. Cells were co-transfected with the constructed luciferase reporter vectors (1-2 μg) and 50 mM miR-199a-5p or matched controls using Lipofectamine 2000. At 48 h post-transfection, luciferase activity was evaluated using a Dual-Luciferase Reporter Detection System (Promega Corporation). The relative luciferase activity was expressed as the ratio of firefly luciferase to *Renilla* luciferase activity.

Statistical analyses. Statistical analyses using SPSS 13.0 software (SPSS, Inc.) were performed using a two-tailed unpaired t-test for comparing clinicopathological characteristics between patients with AMI (n=19) and healthy subjects (n=23; Table I), or one-way analysis of variance followed by Bonferroni post hoc tests for multiple comparisons. Data were presented as the mean ± standard deviation of at least three experiments. P<0.05 was considered to indicate a statistically significant difference.

Results

miR-199a-5p is upregulated in the plasma of patients with AMI and OGD/R-treated H9c2 cells. The expression levels of miR-199a-5p were determined in plasma obtained from male patients with AMI (n=19) and healthy subjects (n=23) to investigate its potential roles in patients. The clinicopathological data of patients and controls are presented in Table I. There were no significant differences between patients with AMI and the control group for any of the reported variables, including age, hypertension, hyperlipidemia, diabetes, LDL cholesterol and blood pressure (P>0.05). Conversely, RT-qPCR analysis revealed that the plasma levels of miR-199a-5p were significantly increased in patients with AMI compared with in healthy controls (7.118±0.08 vs. 7.516±0.113; P=0.007; Fig. 1A).

To further investigate whether the expression of miR-199a-5p is associated with AMI, RT-qPCR analysis was conducted in the OGD/R H9c2 model; it was revealed that the expression of miR-199a-5p was upregulated in the OGD/R-induced H9c2 cells compared with control cells (P<0.01; Fig. 1B). These findings suggested that the expression of miR-199a-5p may serve important roles in OGD/R-induced injury.

miR-199a-5p mimic promotes OGD/R-induced cytotoxicity in H9c2 cells. To determine the effects of the miR-199a-5p overexpression on OGD/R-induced injury, H9c2 cells were transfected with miR-199a-5p mimic or SC. RT-qPCR analysis revealed that transfection with miR-199a-5p mimic significantly increased its expression in H9c2 cells following transfection for 24 h compared with NC-transfected cells (P<0.05; Fig. 2A).

MTS and LDH assays revealed that miR-199a-5p mimic significantly decreased the viability of (P<0.01), and promoted LDH leakage from (P<0.05) OGD/R-treated H9c2 cells compared with the SC (Fig. 2B and C). Additionally, western blot analysis demonstrated that the upregulation of miR-199a-5p significantly inhibited the expression of HIF-1α and the p-GSK3β/GSK3β protein ratio in OGD/R-treated H9c2 cells (P<0.01; Fig. 2D).

Knockdown of miR-199a-5p attenuates cytotoxicity in OGD/R-treated H9c2 cells. To further determine the role of miR-199a-5p in OGD/R-treated H9c2 cells and investigate whether miR-199a-5p knockdown may alleviate the OGD/R-induced myocardial cytotoxicity, OGD/R-induced H9c2 cells were transfected with miR-199a-5p inhibitor or SC. Following transfection with inhibitor for 24 h, the expression of miR-199a-5p was significantly reduced compared with SC (P<0.001; Fig. 3A). The effects of miR-199a-5p downregulation on the viability, cytotoxicity, apoptosis, and ΔΨm of OGD/R-treated cells was subsequently investigated. As demonstrated using an MTS assay, the OGD/R-induced decrease in H9c2 cell viability was significantly rescued following transfection with miR-199a-5p inhibitor for 24 h, compared with OGD/R-treated H9c2 cells (Fig. 3B). Similarly, compared with the OGD/R-treated group, miR-199a-5p inhibitor significantly suppressed the OGD/R-induced leakage of LDH from H9c2 cells (P<0.05; Fig. 3C). Furthermore, TUNEL staining revealed that miR-199a-5p inhibitor significantly decreased the number of apoptotic H9c2 cells compared with the OGD/R-treated group (P<0.01; Fig. 3D and E). JC-1 was used to detect alterations in the ΔΨm, which indirectly reflects the degree of mitochondrial permeability transition pore (mPTP) opening. Compared with the OGD/R-treated group, transfection with the miR-199a-5p inhibitor significantly rescued OGD/R-induced ΔΨm depolarization in H9c2 cells (Fig. 3F and G). In addition, western blot analysis revealed that knockdown of miR-199a-5p in OGD/R-induced H9c2 cells significantly rescued the expression of HIF-1α and the phosphorylation of GSK3β (P<0.01; Fig. 3H). Overall, these findings indicated that miR-199a-5p promoted OGD/R-induced apoptosis, LDH leakage and alterations in the ΔΨm in H9c2 cells, potentially via regulation of the expression of HIF-1α and p-GSK3β.

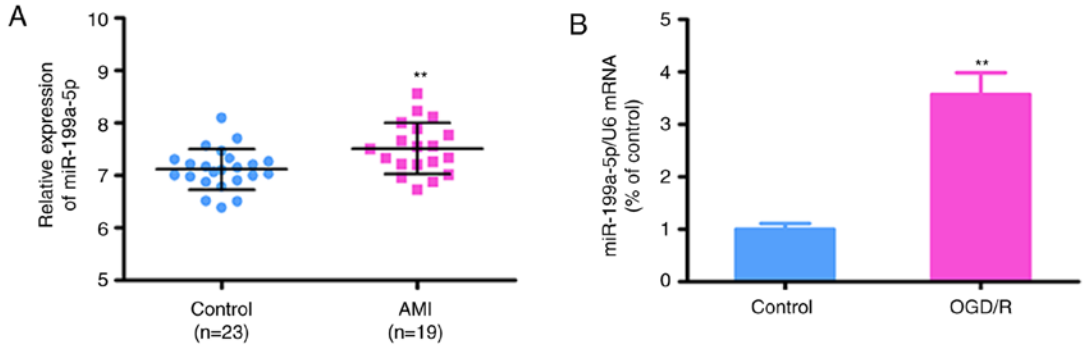

Figure 1. miR-199a-5p expression is upregulated in plasma obtained from patients with AMI and H9c2 cells exposed to OGD/R. (A) miR-199a-5p expression in plasma samples collected from patients <24 h following the onset of AMI (n=19) and healthy controls (n=23). The data are presented as the mean ± standard deviation. **P<0.01 vs. Control. (B) miR-199a-5p expression in H9c2 cells exposed to OGD/R. U6 was used as an internal control. Data are presented as the mean ± standard deviation. **P<0.01 vs. control. miR-199a-5p, microRNA-199a-5p; AMI, acute myocardial infarction; OGD/R, oxygen-glucose deprivation and reperfusion.

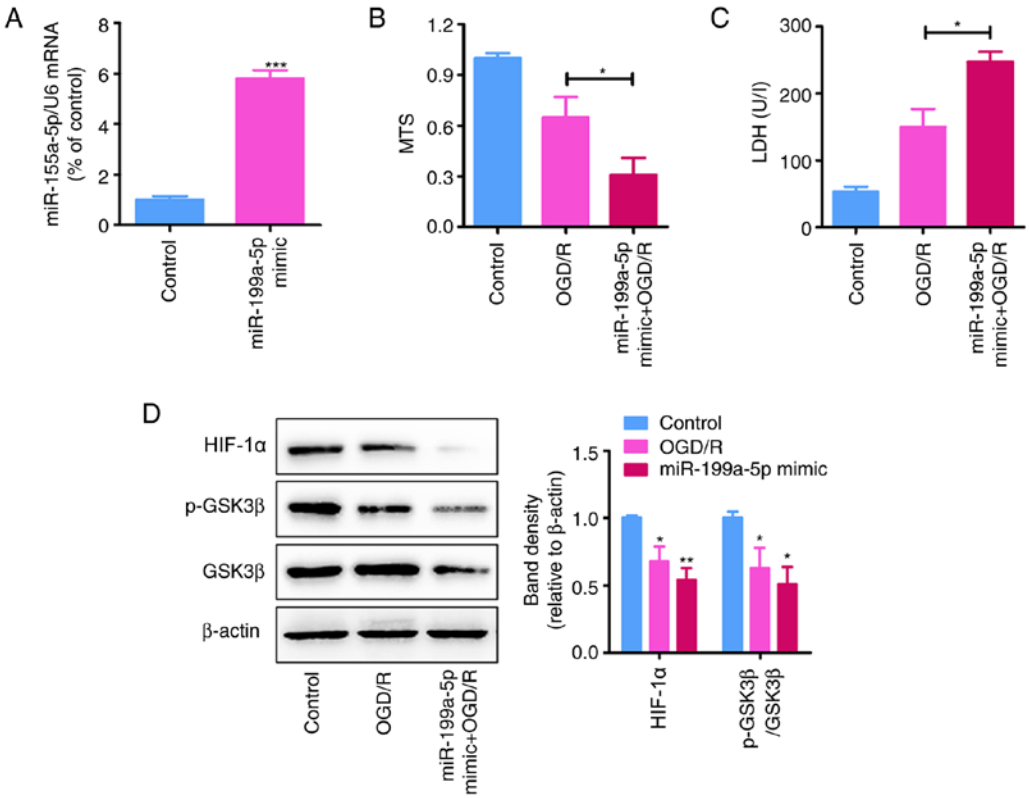

Figure 2. miR-199a-5p overexpression increases OGD/R-induced cytotoxicity in H9c2 cells. (A) miR-199a-5p expression in H9c2 cells transfected with miR-199a-5p mimic or SC (200 nM) under normoxia for 24 h, as determined by reverse transcription-quantitative PCR analysis. ***P<0.001 vs. control. (B) MTS and (C) LDH assays of control and OGD/R-treated H9c2 cells transfected with miR-199a-5p mimic or control (n=3). *P<0.05. (D) Expression of HIF-1α, GSK3β and p-GSK3β (Ser9) in OGD/R-treated H9c2 cells transfected with miR-199a-5p mimic or control, as determined by western blotting. Protein expression levels of HIF-1α and the relative p-GSK3β/GSK3β protein ratio were quantified using ImageJ software and normalized to β-actin. *P<0.05, **P<0.01 vs. SC. Data are presented as the mean ± standard deviation. Each experiment was repeated three times. miR-199a-5p, microRNA-199a-5p; SC/control, scrambled control; OGD/R, oxygen-glucose deprivation and reperfusion; LDH, lactate dehydrogenase; HIF-1α, hypoxia-inducible factor-1α; p-, phosphorylated; GSK3β, glycogen synthase kinase 3β.

Knockdown of miR-199a-5p attenuates OGD/R-induced cytotoxicity in H9c2 cells by regulating the HIF-1α-GSK3β pathway. HIF-1α was reported to be a putative target of miR-199a-5p (17,18), and the p-GSK3β signaling serves as an effector of cardioprotection (22); therefore, whether p-GSK3β is an effector of HIF-1α was investigated. To determine the molecular mechanisms underlying the role of miR-199a-5p as a proapoptotic factor in the OGD/R model, TargetScan was used to predict the potential targets of miR-199a-5p. HIF-1α was predicted to be a candidate target gene of miR-199a-5p, with complementary binding sites of miR-199a-5p identified in the 3'-UTR of HIF-1α (Fig. 3I). To validate the prediction of direct binding between miR-199a-5p and HIF-1α, a luciferase reporter assay was performed. As presented in Fig. 3J, co-transfection with miR-199a-5p and HIF-1α (WT) significantly reduced the luciferase activity (P<0.01), whereas

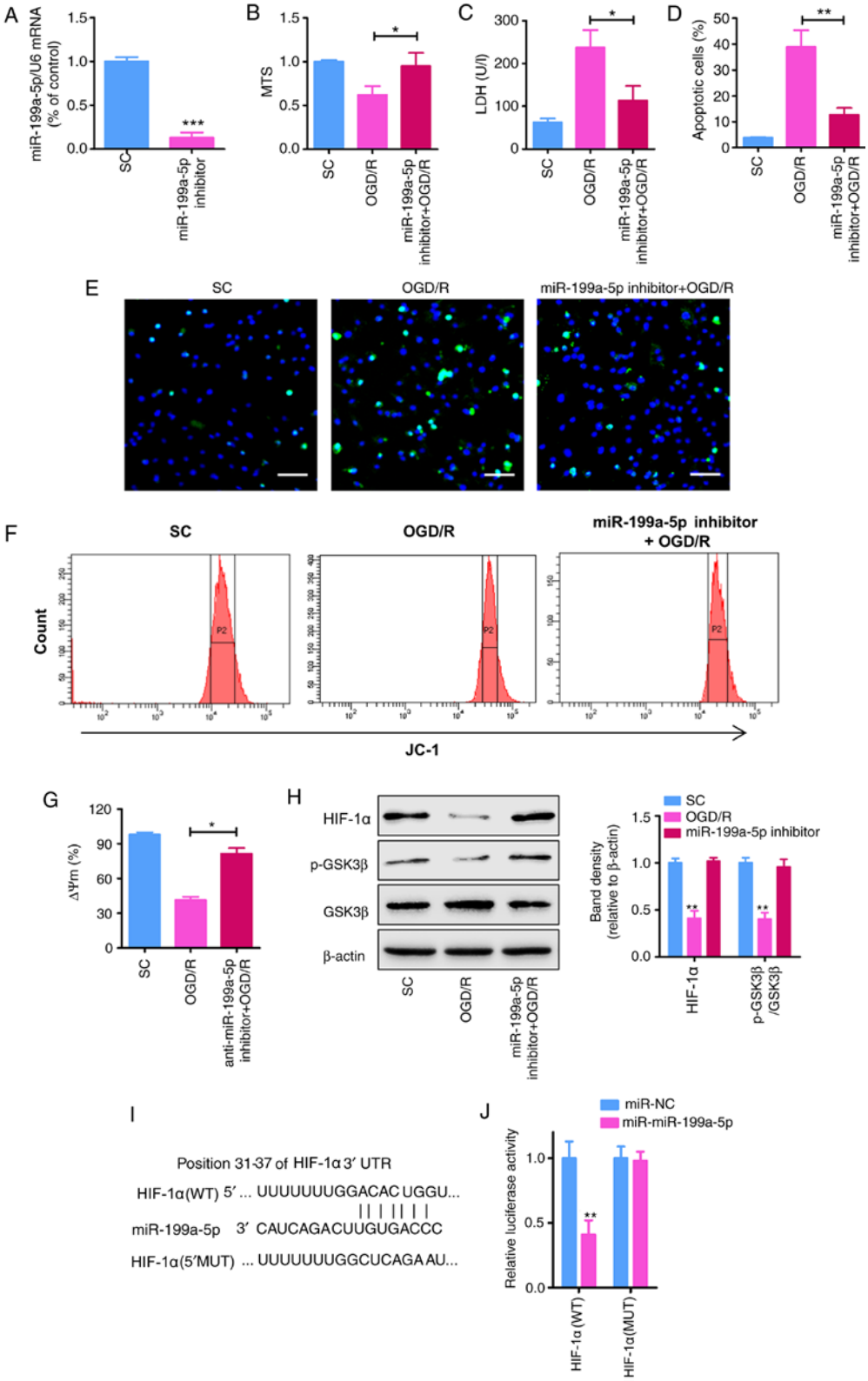

Figure 3. miR-199a-5p downregulation reduces OGD/R-induced cytotoxicity and increases the expression of HIF-1α and p-GSK3β in H9c2 cells. (A) Expression of miR-199a-5p in H9c2 cells transfected with miR-199a-5p inhibitor or SC (200 nM) for 24 h, as determined by reverse transcription-quantitative PCR analysis. ***P<0.001 vs. SC. (B) MTS and (C) LDH assays of H9c2 cells treated with OGD/R and transfected with miR-199a-5p inhibitor or SC. *P<0.05. (D) Percentage of apoptosis H9c2 cells following OGD/R treatment, as determined by a TUNEL assay. **P<0.01. (E) Images of TUNEL staining for the detection of apoptosis of OGD/R-injured cardiomyocytes. Scale bar, 50 μm. (F) Flow cytometric analysis of the ΔΨm in H9c2 cells. (G) Analysis of the ΔΨm determined by JC-1 detection. *P<0.05 vs.OGD/R. (H) Western blotting and quantification of HIF-1α expression and the relative p-GSK3β/GSK3β protein ratio. **P<0.01 vs. SC. (I) Predicted binding sites between miR-199a-5p and HIF-1α mRNA via complementary base-pairs. Luciferase reporter plasmids containing WT or MUT 3'-UTRs of HIF-1α were constructed. (J) Luciferase reporter assays were performed to detect the luciferase activity in 293A cells following co-transfection with miR-199a-5p or miR-NC, and HIF-1α (WT) or HIF-1α (MUT) reporter plasmids. **P<0.01 vs. miR-NC. Data are presented as the mean ± standard deviation of three independent experiments. miR-199a-5p, microRNA-199a-5p; SC, scrambled control; OGD/R, oxygen-glucose deprivation and reperfusion; LDH, lactate dehydrogenase; ΔΨm, mitochondrial membrane potential; HIF-1α, hypoxia-inducible factor-1α; p-, phosphorylated; GSK3β, glycogen synthase kinase 3β; UTR, untranslated region; WT, wild-type; MUT, mutant; miR-NC, miR negative control.

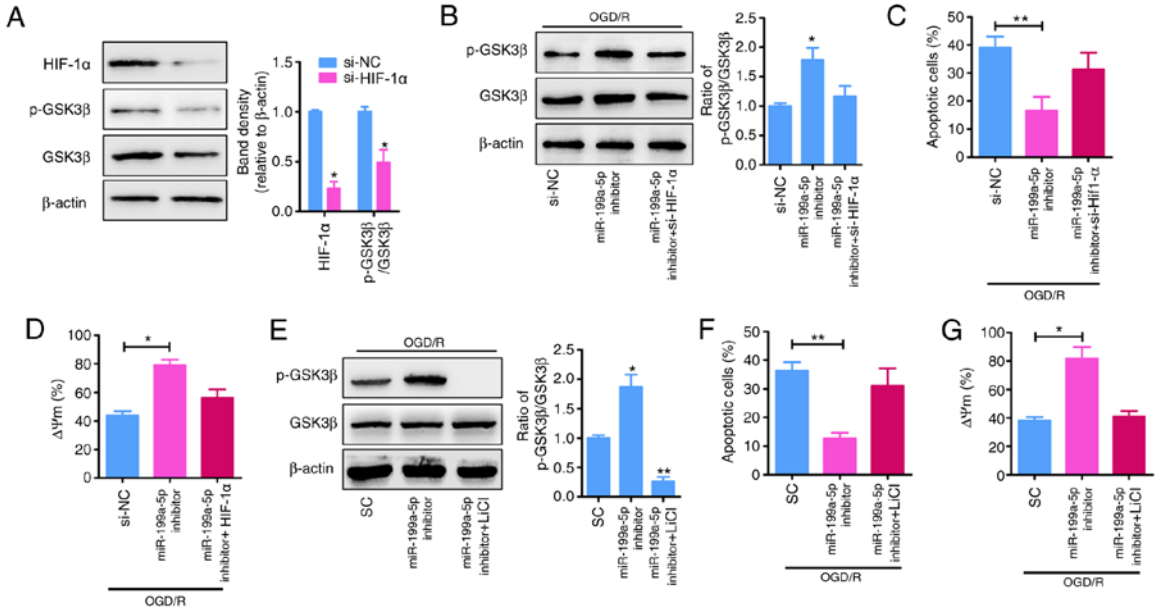

Figure 4. miR-199a-5p inhibitor mediates protection against OGD/R-induced injury by upregulating the expression of HIF-1α and p-GSK3β. (A) Analysis of HIF-1α levels and the relative p-GSK3β/GSK3β protein ratio in H9c2 cells transfected with si-NC or si-HIF-1α. *P<0.05 vs. si-NC. (B) H9c2 cells were treated with OGD/R and transfected with miR-199a-5p inhibitor in the presence or absence of si-HIF-1α. The cell lysates were analyzed by western blotting for GSK3β and p-GSK3β; expression was quantified by ImageJ software and normalized to β-actin. *P<0.05 vs. si-NC. (C) Apoptosis and (D) $\Delta\Psi_m$ were analyzed by TUNEL and flow cytometry analyses, respectively. *P<0.05, **P<0.01. (E) OGD/R-treated H9c2 cells were transfected with miR-199a-5p inhibitor in the presence or absence of LiCl. The cell lysates were analyzed by western blotting for GSK3β and p-GSK3β; expression was quantified by ImageJ software and normalized to β-actin. *P<0.05, **P<0.01 vs. SC. (F) Apoptosis and (G) ΔΨm were analyzed by TUNEL and flow cytometry analyses, respectively. *P<0.05, **P<0.01. Data are presented as the mean ± standard deviation of four independent experiments. HIF-1α, hypoxia-inducible factor-1α; p-, phosphorylated; GSK3β, glycogen synthase kinase 3β; si-, short interfering RNA; NC, negative control; OGD/R, oxygen-glucose deprivation and reperfusion; miR-199a-5p, microRNA-199a-5p; ΔΨm, mitochondrial membrane potential; SC, scrambled control.

co-transfection with miR-199a-5p and HIF-1α (mut) did not significantly alter luciferase activity in 293A cells. To determine the effects of HIF-1α on p-GSK3β signaling in H9c2 cells under OGD/R, the expression of HIF-1α was inhibited via transfection of H9c2 cells with siRNA-HIF-1α, which significantly reduced the expression of HIF-1α and p-GSK3β compared with si-NC (P<0.05; Fig. 4A and B). Furthermore, the reduced apoptosis (P<0.01; Fig. 4C and F) and ΔΨm depolarization (Fig. 4D and G) following miR-199a-5p knockdown in OGD/R-induced H9c2 cells was significantly attenuated by the downregulation of HIF-1α expression (Fig. 4B) or the inhibition of p-GSK3β expression via treatment with LiCl (a specific inhibitor of p-GSK3β; P<0.01; Fig. 4E). Collectively, these results suggested that miR-199a-5p mediates OGD/R-induced cytotoxicity in H9c2 cells, partially by suppressing the expression of HIF-1α and the downstream phosphorylation of GSK3β.

Downregulation of miR-199a-5p contributes to the binding of p-GSK3β to ANT in the mPTP. The opening of the mPTP induces apoptotic cell death during I/R (23). To determine the effects of the downregulation of miR-199a-5p on the opening of the mPTP, the OGD/R-induced formation of protein complexes between two main mPTP components, ANT and Cyp-D was detected via IP assays. It was demonstrated that miR-199a-5p downregulation notably decreased the formation of ANT-Cyp-D complexes (Fig. 5A, lane 2 vs. 3), whereas the interaction between ANT and Cyp-D was restored when OGD/R-treated cells were co-transfected with si-HIF-1α and miR-199a-5p inhibitor (Fig. 5A, lane 3 vs. 4). Furthermore, the binding of ANT and p-GSK3β was analyzed by an IP assay using anti-p-GSK3β antibodies. As presented in Fig. 5B, miR-199a-5p downregulation increased the binding of p-GSK3β to ANT, indicating that miR-199a-5p inhibitor-induced interactions between p-GSK3β and ANT inhibited OGD/R-induced interactions between ANT and Cyp-D (Fig. 5B, lane 2 vs. 3). Similarly, OGD/R-induced H9c2 cells were treated with miR-199a-5p inhibitor and LiCl, which also notably promoted the interaction between Cyp-D and ANT (Fig. 5C, lane 3 vs. 4). The binding of p-GSK3β to the mitochondrial membrane was further characterized via immunofluorescence staining. In OGD/R + miR-199a-5p inhibitor-treated H9c2 cells, p-GSK3β (red) and ANT (green) were localized predominately in the mitochondria (yellow; Fig. 5D), whereas LiCl treatment notably decreased the binding of p-GSK3β to ANT in the mPTP. These findings indicated that the effect of miR-199a-5p knockdown on the cytotoxicity of OGD/R-induced H9c2 cells is mediated by upregulating the expression of HIF-1α and p-GSK3β, promoting the interaction between p-GSK3β and ANT, which, in turn, reduces the interaction between ANT and Cyp-D, and subsequently contributing to the suppression of mPTP opening.

Discussion

Myocardial I/R injury is an inevitable consequence of the treatment of ischemic heart disease. Thus, the protection of I/R-exposed cardiac tissue is a major therapeutic challenge in modern cardiology (24). The present study detected the plasma levels of miR-199a-5p in patients with AMI and in an

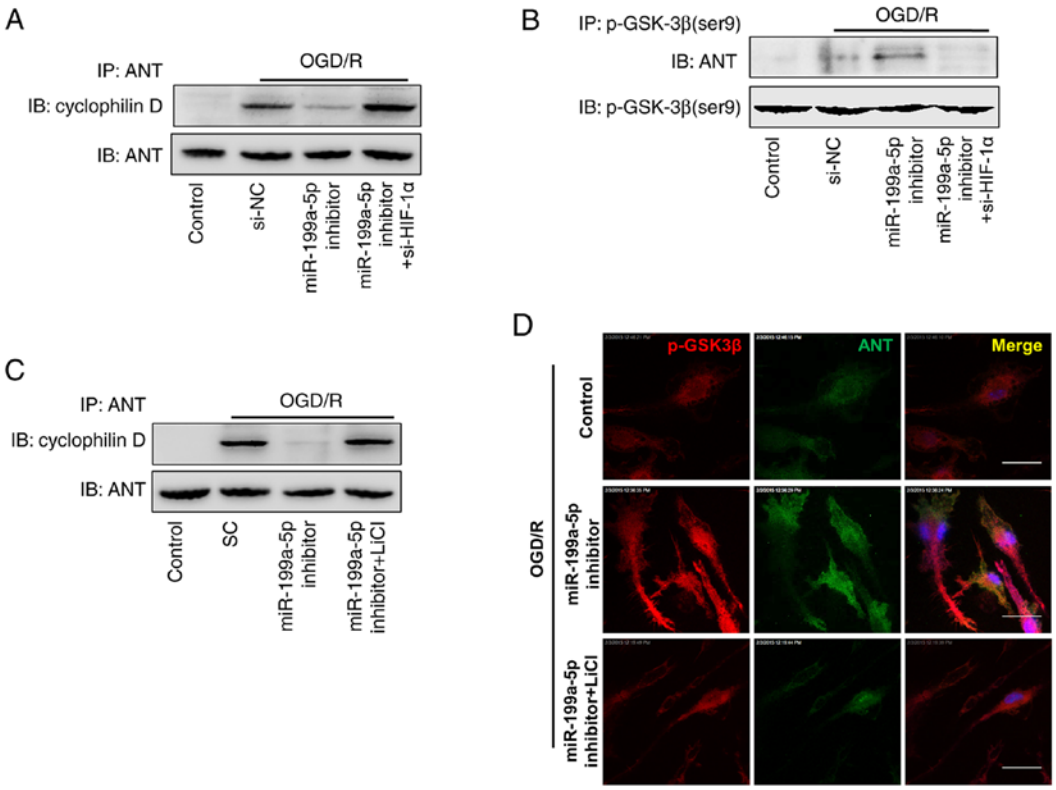

Figure 5. Interactions between p-GSK3β and ANT following miR-199a-5p downregulation inhibit the formation of the ANT-Cyp-D complex. H9c2 cells were transfected with si-NC, miR-199a-5p inhibitor, or co-transfected with miR-199a-5p inhibitor and si-HIF-1 under OGD/R conditions. Detection of ANT coimmunoprecipitated with (A) Cyp-D or (B) p-GSK3β by western blotting. (C) H9c2 cells were transfected with SC, or miR-199a-5p inhibitor in the presence or absence of LiCl treatment under OGD/R conditions. Detection of ANT coimmunoprecipitated with Cyp-D by western blotting. (D) Colocalization of ANT with p-GSK3β in treated H9c2 cells was analyzed by confocal fluorescence microscopy. Nuclei were stained with DAPI. Scale bar, 10 μm. IP, immunoprecipitation; ANT, adenine nucleotide transferase; OGD/R, oxygen-glucose deprivation and reperfusion; Control, untreated H9c2 cells; si-, short interfering RNA; NC, negative control; miR-199a-5p, microRNA-199a-5p; HIF-1α, hypoxia-inducible factor-1α; p-, phosphorylated; GSK3β, glycogen synthase kinase 3β; SC, scrambled control; Cyp-D, cyclophilin D.

OGD/R-induced H9c2 cell model, in addition to the effects of miR-199a-5p on OGD/R-induced cytotoxicity in H9c2 cells. OGD/R-treated H9c2 cells were transfected with miR-199a-5p mimic or inhibitor to overexpress or knockdown miR-199a-5p, as previously described (16). It was observed that the upregulation of miR-199a-5p inhibited cell survival and promoted LDH leakage from OGD/R-induced H9c2 cells, whereas miR-199a-5p knockdown promoted the viability, and inhibited the apoptosis and alterations in the ΔΨm of OGD/R-treated H9c2 cells, potentially by increasing the expression of HIF-1α and p-GSK3β, and promoting the interaction between p-GSK3β and ANT, thereby suppressing the OGD/R-induced interaction of ANT with Cyp-D and opening of the mPTP.

miRNAs are involved in cardiac pathological processes, including cardiac hypertrophy (25), arrhythmogenesis (26) and heart failure (27). Increasing evidence indicates that miRNAs may be potential therapeutic targets against myocardial I/R. Reportedly, miR-199a-3p is upregulated in injured mouse kidneys following renal I/R (28). Additionally, miRNA-199a overexpression decreased sirtuin 1 (Sirt1) levels, whereas silencing miRNA-199a using antisense oligonucleotides or by hypoxic preconditioning increased Sirt1 expression (19). A previous study suggested that inhibition of the mPTP opening may be a novel target for cardioprotective drugs against myocardial infarction (23). Based on this finding, it was investigated as to r whether miR-199a-5p exhibited cardioprotective effects via regulation of mPTP opening. It was demonstrated that miR-199a-5p inhibitor effectively suppressed cell apoptosis and LDH leakage, and rescued cell viability and the $\Delta\Psi_m$ following OGD/R. Additionally, it was observed that miR-199a-5p inhibitor significantly upregulated the expression of HIF-1α and p-GSK3β. The inhibition of p-GSK3β modulated the opening of the mPTP, contributing to cardiac injury during myocardial I/R (29).

The present study determined that miR-199a-5p knockdown regulated HIF-1α activation-mediated cardioprotection in OGD/R-injured H9c2 cells. Of note, the knockdown of HIF-1α reversed the protective effects of the miR-199a-5p inhibitor on OGD/R-injured H9c2 cells via by decreasing p-GSK3β expression (Fig. 4B). The activation of GSK3β via dephosphorylation during prolonged ischemia has been reported to be protective; however, the inactivation of GSK3β via phosphorylation during the reperfusion phase may also be protective (30). The protein stability of HIF-1α and the phosphorylation of GSK3β are cardioprotective against I/R (31). The stabilization of HIF-1α in the murine heart may inhibit mPTP opening following I/R (32). In addition, the phosphorylation of GSK3β inhibited mPTP opening following the I/R injury of cardiomyocytes (33). Of note, in non-neuronal cells, increased serine phosphorylation and subsequent inactivation of GSK3β is associated with increased HIF-1α expression (34). Furthermore, GSK3β phosphorylation is associated with HIF-1α expression in H9c2 cells (35).

Juhaszova *et al* (36) first reported that the activity of GSK3β sets a threshold for mPTP opening in cardiomyocytes, and that the threshold for the reactive oxygen species-induced opening of the mPTP is increased by the inhibitory phosphorylation of GSK3β. The molecular mechanisms via which the inactivation of GSK3β (or its phosphorylation at Ser9) increases the threshold for mPTP opening remains unclear; however, it appears that the suppression of ANT-Cyp-D interactions via the binding of p-GSK3β to ANT contributes to the elevation of the threshold (33,36,37). The present findings suggested that the knockdown of miR-199a-5p reduced the interaction between ANT and Cyp-D, indicating that inactivation of GSK3β via its phosphorylation at Ser9 dismantles the mPTP complex. It has been reported that pharmacological inhibitors of GSK3β limit the infarct size when administered prior to I/R injury (38), suggesting fine-tuned mechanisms via which the altered phosphorylation GSK3 serves complex roles in mPTP opening in cardiomyocytes.

Collectively, the present findings suggested that the upregulation of miR-199a-5p expression contributed to I/R injury in cardiomyocytes. Knockdown of miR-199a-5p protected against I/R-induced cardiomyocyte apoptosis by targeting the HIF-1α-GSK3β-mPTP axis, which may be a potential target for therapeutic intervention in patients with AMI.

Acknowledgements

Not applicable.

Funding

The present study was supported by the Foundation of the Second Hospital of Hebei Medical University (grant no. 2h201804).

Availability of data and materials

The datasets used and/or analyzed during the current study are available from the corresponding author on reasonable request.

Authors' contributions

DWL, YNZ, HJH, PQZ and WC conducted the experiments and data collection, and interpreted the data. DWL was involved in the design and coordination of experiments, the acquisition and analysis of data, and drafting the manuscript. WC made substantial contributions to the design, analysis and interpretation of data.

Ethics approval and consent to participate

The present study was approved by the Ethical Committee of Second Hospital of Hebei Medical University. Experimental procedures were implemented in according to the guidelines and regulations of Hebei Medical University. Patients provided written informed consent.

Patient consent for publication

Not applicable.

Competing interests

The authors declare that they have no competing interests.

References

1. Hausenloy DJ and Yellon DM: Targeting myocardial reperfusion injury-the search continues. N Engl J Med 373: 1073-1075, 2015.
2. Pagliaro P, Moro F, Tullio F, Perrelli MG and Penna C: Cardioprotective pathways during reperfusion: Focus on redox signaling and other modalities of cell signaling. Antioxid Redox Signal 14: 833-850, 2011.
3. Murry CE, Jennings RB and Reimer KA: Preconditioning with ischemia: A delay of lethal cell injury in ischemic myocardium. Circulation 74: 1124-1136, 1986.
4. Yue R, Xia X, Jiang J, Yang D, Han Y, Chen X, Cai Y, Li L, Wang WE and Zeng C: Mitochondrial DNA oxidative damage contributes to cardiomyocyte Ischemia/Reperfusion-injury in rats: Cardioprotective role of lycopene. J Cell Physiol 230: 2128-2141, 2015.
5. Kaczorowski DJ, Nakao A, McCurry KR and Billiar TR: Toll-like receptors and myocardial ischemia/reperfusion, inflammation, and injury. Curr Cardiol Rev 5: 196-202, 2009.
6. Prasad A, Stone GW, Holmes DR and Gersh B: Reperfusion injury, microvascular dysfunction, and cardioprotection: The 'dark side' of reperfusion. Circulation 120: 2105-2112, 2009.
7. Laina A, Gatsiou A, Georgiopoulos G, Stamatelopoulos K and Stellos K: RNA therapeutics in cardiovascular precision medicine. Front Physiol 9: 953, 2018.
8. Zhu H and Fan GC: Role of microRNAs in the reperfused myocardium towards post-infarct remodelling. Cardiovasc Res 94: 284-292, 2012.
9. Bian B, Yu XF, Wang GQ and Teng TM: Role of miRNA-1 in regulating connexin 43 in ischemia-reperfusion heart injury: A rat model. Cardiovasc Pathol 27: 37-42, 2017.
10. Chen X, Zhang L, Su T, Li H, Huang Q, Wu D, Yang C and Han Z: Kinetics of plasma microRNA-499 expression in acute myocardial infarction. J Thorac Dis 7: 890-896, 2015.
11. Zhang XH, Zheng B, Han M, Miao SB and Wen JK: Synthetic retinoid Am80 inhibits interaction of KLF5 with RAR alpha through inducing KLF5 dephosphorylation mediated by the PI3K/Akt signaling in vascular smooth muscle cells. FEBS Lett 583: 1231-1236, 2009.
12. Song CL, Liu B, Diao HY, Shi YF, Zhang JC, Li YX, Liu N, Yu YP, Wang G, Wang JP and Li Q: Down-regulation of microRNA-320 suppresses cardiomyocyte apoptosis and protects against myocardial ischemia and reperfusion injury by targeting IGF-1. Oncotarget 7: 39740-39757, 2016.
13. Su S, Luo, Liu X, Liu J, Peng F, Fang C and Li B: miR-494 up-regulates the PI3K/Akt pathway via targetting PTEN and attenuates hepatic ischemia/reperfusion injury in a rat model. Biosci Rep 37: pii: BSR20170798, 2017.
14. Liu Y, Liu G, Zhang H and Wang J: MiRNA-199a-5p influences pulmonary artery hypertension via downregulating Smad3. Biochem Biophys Res Commun 473: 859-866, 2016.
15. Wang D, Li Z, Zhang Y, Wang G, Wei M, Hu Y, Ma S, Jiang Y, Che N, Wang X, *et al*: Targeting of microRNA-199a-5p protects against pilocarpine-induced status epilepticus and seizure damage via SIRT1-p53 cascade. Epilepsia 57: 706-716, 2016.
16. Zuo Y, Wang Y, Hu H and Cui W: Atorvastatin protects myocardium against ischemia-reperfusion injury through inhibiting miR-199a-5p. Cell Physiol Biochem 39: 1021-1030, 2016.
17. Schnitzer SE, Schmid T, Zhou J, Eisenbrand G and Brüne B: Inhibition of GSK3beta by indirubins restores HIF-1alpha accumulation under prolonged periods of hypoxia/anoxia. FEBS Lett 579: 529-533, 2005.
18. Yang X, Lei S, Long J, Liu X and Wu Q: MicroRNA-199a-5p inhibits tumor proliferation in melanoma by mediating hif-1α. Mol Med Rep 13: 5241-5249, 2016.
19. Rane S, He M, Sayed D, Vashistha H, Malhotra A, Sadoshima J, Vatner DE, Vatner SF and Abdellatif M: Downregulation of miR-199a derepresses hypoxia-inducible factor-1alpha and Sirtuin 1 and recapitulates hypoxia preconditioning in cardiac myocytes. Circ Res 104: 879-886, 2009.
20. Livak KJ and Schmittgen TD: Analysis of relative gene expression data using real-time quantitative PCR and the 2(-Delta Delta C(T)) method. Methods 25: 402-408, 2001.

21. Nishihara M, Miura T, Miki T, Tanno M, Yano T, Naitoh K, Ohori K, Hotta H, Terashima Y and Shimamoto K: Modulation of the mitochondrial permeability transition pore complex in GSK-3β-mediated myocardial protection. J Mol Cell Cardiol 43: 564-570, 2007.
22. Chen L, Cai P, Cheng Z, Zhang Z and Fang J: Pharmacological postconditioning with atorvastatin calcium attenuates myocardial ischemia/reperfusion injury in diabetic rats by phosphorylating GSK3β. Exp Ther Med 14: 25-34, 2017.
23. Gyulkhandanyan AV, Mutlu A, Freedman J and Leytin V: Mitochondrial permeability transition pore (MPTP)-dependent and -independent pathways of mitochondrial membrane depolarization, cell shrinkage and microparticle formation during platelet apoptosis. Br J Haematol 169: 142-150, 2015.
24. Sivaraman V and Yellon DM: Pharmacologic therapy that simulates conditioning for cardiac ischemic/reperfusion injury. J Cardiovasc Pharmacol Ther 19: 83-96, 2014.
25. Heggermont WA, Papageorgiou AP, Quaegebeur A, Deckx S, Carai P, Verhesen W, Eelen G, Schoors S, van Leeuwen R, Alekseev S, *et al*: Inhibition of MicroRNA-146a and overexpression of its target dihydrolipoyl succinyltransferase protect against pressure overload-induced cardiac hypertrophy and dysfunction. Circulation 136: 747-761, 2017.
26. Danielson LS, Park DS, Rotllan N, Chamorro-Jorganes A, Guijarro MV, Fernandez-Hernando C, Fishman GI, Phoon CK and Hernando E: Cardiovascular dysregulation of miR-17-92 causes a lethal hypertrophic cardiomyopathy and arrhythmogenesis. FASEB J 27: 1460-1467, 2013.
27. Verjans R, Peters T, Beaumont FJ, van Leeuwen R, van Herwaarden T, Verhesen W, Munts C, Bijnen M, Henkens M, Diez J, *et al*: MicroRNA-221/222 family counteracts myocardial fibrosis in pressure overload-induced heart failure. Hypertension 71: 280-288, 2018.
28. Godwin JG, Ge X, Stephan K, Jurisch A, Tullius SG and Iacomini J: Identification of a microRNA signature of renal ischemia reperfusion injury. Proc Natl Acad Sci USA 107: 14339-14344, 2010.
29. Gomez L, Paillard M, Thibault H, Derumeaux G and Ovize M: Inhibition of GSK3beta by postconditioning is required to prevent opening of the mitochondrial permeability transition pore during reperfusion. Circulation 117: 2761-2768, 2008.
30. Zhai P, Sciarretta S, Galeotti J, Volpe M and Sadoshima J: Differential roles of GSK-3β during myocardial ischemia and ischemia/reperfusion. Circ Res 109: 502-511, 2011.
31. Nguyen T, Wong R, Wang G, Gucek M, Steenbergen C and Murphy E: Acute inhibition of GSK causes mitochondrial remodeling. Am J Physiol Heart Circ Physiol 302: H2439-H2445, 2012.
32. Wu J, Ke X, Fu W, Gao X, Zhang H, Wang W, Ma N, Zhao M, Hao X and Zhang Z: Inhibition of hypoxia-induced retinal angiogenesis by specnuezhenide, an effective constituent of ligustrum lucidum Ait., through suppression of the HIF-1α/VEGF signaling pathway. Molecules 21: pii: E1756, 2016.
33. Wang S, Zhang F, Zhao G, Cheng Y, Wu T, Wu B and Zhang YE: Mitochondrial PKC-ε deficiency promotes I/R-mediated myocardial injury via GSK3β-dependent mitochondrial permeability transition pore opening. J Cell Mol Med 2: 2009-2021, 2017.
34. Flügel D, Görlach A and Kietzmann T: GSK-3β regulates cell growth, migration, and angiogenesis via Fbw7 and USP28-dependent degradation of HIF-1α. Blood 119: 1292-1301, 2012.
35. Huang X, Zuo L, Lv Y, Chen C, Yang Y, Xin H, Li Y and Qian Y: Asiatic acid attenuates myocardial ischemia/reperfusion injury via Akt/GSK-3β/HIF-1α signaling in rat H9c2 cardiomyocytes. Molecules 21: E1248, 2016.
36. Juhaszova M, Wang S, Zorov DB, Nuss HB, Gleichmann M, Mattson MP and Sollott SJ: The identity and regulation of the mitochondrial permeability transition pore: Where the known meets the unknown. Ann NY Acad Sci 1123: 197-212, 2010.
37. Zhu H, Ding Y, Xu X, Li M, Fang Y, Gao B, Mao H, Tong G, Zhou L and Huang J: Prostaglandin E1 protects coronary microvascular function via the glycogen synthase kinase 3β-mitochondrial permeability transition pore pathway in rat hearts subjected to sodium laurate-induced coronary microembolization. Am J Transl Res 9: 2520-2534, 2017.
38. Obame FN, Plin-Mercier C, Assaly R, Zini R, Dubois-Randé JL, Berdeaux A and Morin D: Cardioprotective effect of morphine and a blocker of glycogen synthase kinase 3 beta, SB216763 [3-(2,4-dichlorophenyl)-4(1-methyl-1H-indol-3-yl)-1H-pyrrole-2,5-dione], via inhibition of the mitochondrial permeability transition pore. J Pharmacol Exp Ther 326: 252-258, 2008.